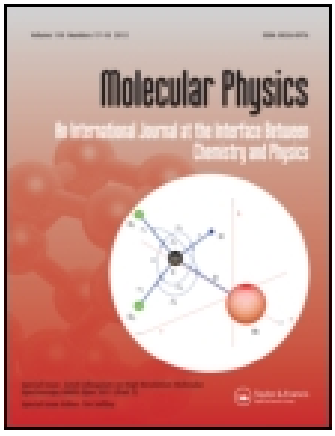

Molecular Physics: An International Journal at the Interface Between Chemistry and Physics
Publication details, including instructions for authors and subscription information:
http://www.tandfonline.com/loi/tmph20

Theoretical calculations for line-broadening and pressure-shifting in the $\nu_1+\nu_2+\nu_4+\nu_5$ band of acetylene over a range of temperatures

J.P. Bouanich [a] & A. Predoi-Cross [b]

[a] Institut des Sciences Moléculaires d'Orsay (ISMO) , CNRS, Université de Paris-Sud 11, 91405 Orsay cedex , France

[b] Department of Physics and Astronomy , University of Lethbridge, 4401 University Drive , Lethbridge , AB T1K 3M4 , Canada

Published online: 27 Jul 2011.

To cite this article: J.P. Bouanich & A. Predoi-Cross (2011) Theoretical calculations for line-broadening and pressure-shifting in the $\nu_1+\nu_2+\nu_4+\nu_5$ band of acetylene over a range of temperatures, Molecular Physics: An International Journal at the Interface Between Chemistry and Physics, 109:17-18, 2071-2081, DOI: 10.1080/00268976.2011.599342

To link to this article: http://dx.doi.org/10.1080/00268976.2011.599342

Molecular Physics
Vol. 109, Nos. 17–18, 10 September–20 September 2011, 2071–2081

Taylor & Francis
Taylor & Francis Group

INVITED ARTICLE

Theoretical calculations for line-broadening and pressure-shifting in the $\nu_1 + \nu_2 + \nu_4 + \nu_5$ band of acetylene over a range of temperatures

J.P. Bouanich[a] and A. Predoi-Cross[b]*

[a]*Institut des Sciences Moléculaires d'Orsay (ISMO), CNRS, Université de Paris-Sud 11, 91405 Orsay cedex, France;*
[b]*Department of Physics and Astronomy, University of Lethbridge, 4401 University Drive, Lethbridge, AB T1K 3M4, Canada*

(*Received 23 March 2011; final version received 17 June 2011*)

Semiclassical calculations of self-broadening and self-induced pressure shift coefficients in the $\nu_1+\nu_2+\nu_4+\nu_5$ band of C_2H_2 have been performed by considering, in addition to the main electrostatic quadrupole–quadrupole interaction, a simple anisotropic dispersion contribution, leading to results in overall satisfactory agreement with recent measurements [C. Povey, A. Predoi-Cross and D.R. Hurtmans, J. Mol. Spectrosc., **268**, 177 (2011)]. In these calculations we have used the mean relative velocity and also considered the Maxwell–Boltzmann distribution of relative velocities. From the theoretical results obtained at different temperatures ranging from 200 to 350 K, we have determined temperature exponents of the broadenings using a simple power law, as well as coefficients of empirical linear and quadratic temperature dependences for the line shifts. These theoretical exponents and linear coefficients, derived from averaging over the distribution of velocities and from the mean thermal velocity, are significantly different and they are compared with those obtained from measurements of broadening coefficients and line shifts performed in a comparable temperature range [C. Povey, A. Predoi-Cross and D.R. Hurtmans, J. Mol. Spectrosc., **268**, 177 (2011)]. The theoretical variation of the self-shifts with temperature is not linear and can be well fitted by a quadratic polynomial.

Keywords: semiclassical calculations; acetylene; spectral line shapes; pressure broadening; pressure-induced shifts

1. Introduction

Acetylene is a minor constituent of the Earth's atmosphere [2], as well as the planetary atmospheres of Jupiter [3], Saturn [4], Mars [5] and Titan [6]. It has been the subject of several spectroscopic studies, with emphasis on collisional broadening with rare gases [7–10], H_2 or HD [11–13], N_2 and O_2 [14–17]. The self-broadening coefficients of C_2H_2 lines have been studied experimentally and/or theoretically in different absorption bands: ν_5 [17–19], $\nu_4+\nu_5$ [20, 21], $2\nu_4+\nu_5$ and $3\nu_5$ [20], $\nu_1+\nu_5$ [22], $\nu_1+3\nu_3$ [23–25], $\nu_1+\nu_3$ [26–28], $5\nu_3$ [28,29]. The values for self-broadened and pressure-induced shift coefficients have been measured recently over a range of temperatures for transitions with rotational quantum number m ranging between 1 and 20 in the $\nu_1+\nu_2+\nu_4+\nu_5$ band of C_2H_2 [1]. To our knowledge, no such measurements of broadening coefficients and line shifts have previously been reported on this combination band. The spectra were recorded with a three-channel laser spectrometer located at the University of Lethbridge. The analysis was performed using a multispectrum nonlinear least-squares technique. We have compared our results with similar measurements published recently. The experimental conditions of the spectra, analysis procedures and results are given in Ref. [1] and will not be discussed in this paper. For completeness and convenience, a few critical equations from the preceding paper are reconsidered.

In this study we report theoretical results of self-broadening and pressure shift coefficients and their temperature dependences for lines in the $\nu_1+\nu_2+\nu_4+\nu_5$ band of C_2H_2. Semiclassical calculations of these coefficients have been performed using the Robert–Bonamy formalism [30]. Because of the specificities of C_2H_2 interactions, we have only considered, in addition to the strong quadrupole–quadrupole electrostatic potential, a simple anisotropic dispersion contribution with one adjustable parameter. The calculations of self-broadening coefficients at room temperature are similar to those reported in Refs. [18,21] using the mean thermal velocity, but the results have also been obtained from the Maxwell–Boltzmann distribution of velocities. The self-broadening coefficients and self-induced line shifts at 296 K are first compared with experimental results for the R-branch of the $\nu_1+\nu_2+\nu_4+\nu_5$ band of C_2H_2 [1]. Then, they are calculated at four temperatures

*Corresponding author. Email: adriana.predoicross@uleth.ca

ISSN 0026–8976 print/ISSN 1362–3028 online

http://dx.doi.org/10.1080/00268976.2011.599342
http://www.tandfonline.com

(200, 250, 300 and 350 K) and are also compared with those derived from experimental data in the temperature range 213–333 K and extrapolated at these four temperatures, using the room temperature parameters and their temperature dependencies reported in Ref. [1]. The temperature dependence of the broadening coefficients is deduced from a simple power law, whereas an empirical linear as well as a quadratic temperature dependence are assumed for the self-induced line shifts.

The general formulation of the semiclassical formalism and the energy potential considered have been described previously [31,21] and are briefly presented in Section 2. The theoretical results at four temperatures ranging from 200 to 350 K are displayed and compared with experimental data [1] in Section 3. From these results we have derived in Section 4 the temperature exponents of the self-broadening coefficients as well as temperature coefficients of the line shifts, which are finally compared with experimental evaluations.

2. Theoretical model for self-broadening and pressure-induced shift coefficients

2.1. *General formulation*

The pressure broadened half-width γ_{if} and pressure-induced line shift δ_{if} of an isolated $i \rightarrow f$ line ($v_i J_i \rightarrow v_f J_f$) may be expressed as the real and imaginary parts of a complex cross-section σ_{if},

$$\gamma_{if} = \frac{n\bar{v}}{2\pi c} \operatorname{Re} \sigma_{if}, \quad \delta_{if} = \frac{n\bar{v}}{2\pi c} \operatorname{Im} \sigma_{if}, \tag{1}$$

where n is the number density of perturbing molecules and $\bar{v}$ the average relative velocity. σ_{if} is a weighted sum of the cross-sections for each initial rotational state J_2 of the perturber. Within the semiclassical frame and considering the Maxwell–Boltzmann distribution of velocities [32], σ_{if} is usually expressed in terms of the average over all trajectories as

$$\sigma_{if} = \int_0^\infty x\, \mathrm{e}^{-x} \mathrm{d}x \sum_{J_2} \rho_{J_2} \int_0^\infty 2\pi b S_{if}(b, x, J_2) \mathrm{d}b, \tag{2}$$

where $x = [E/(k_B T)]^{1/2} = v/v_p$, E is the initial relative kinetic energy, v the relative velocity and v_p the most probable relative velocity [$v_p = (2k_B T/m)^{1/2}$, m is the reduced mass of the colliding partners]; ρ_{J_2} is the relative population distribution in the $|J_2, v_2 = 0\rangle$ state of the perturber, including the nuclear spin factor $(-1)^{J_2+1} + 2$; S_{if} is the complex differential cross-section representing the collisional efficiency and b is the impact parameter. In the Robert–Bonamy formalism [30], $S(b)$ is expressed in terms of $S_1(b)$ and $S_2(b)$, respectively the first- and second-order terms in the expansion of the scattering matrix,

$$S(b) = 1 - \mathrm{e}^{-S_2(b)} \mathrm{e}^{-iS_1(b)}. \tag{3}$$

$S_1(b)$ (real) is a vibrational dephasing arising from the difference of the isotropic part of the potential in the upper and lower vibrational states of the transition. $S_2(b)$ is complex [$S_2(b) \equiv \operatorname{Re} S_2(b) + i \operatorname{Im} S_2(b)$] and results from the anisotropic part of the potential. The expressions of $S_1(b)$ and $S_2(b)$ in terms of the intermolecular potential may be found in Ref. [30].

For the description of the trajectories where long-range forces dominate, we used an equivalent straight path trajectory [33] around the distance of closest approach r_c, calculated from the isotropic part of the potential, taken as a Lennard–Jones potential.

2.2. *The C_2H_2–C_2H_2 system*

Because of the C_2H_2 symmetry, the self-broadening coefficient has a dominant quadrupole–quadrupole contribution. Therefore, the anisotropic potential generally used in the calculations has been generally limited to this interaction in which we have added a simple dispersion contribution [18] according to

$$V_{\text{aniso}} = V_{Q_1Q_2} - 4\varepsilon A_2 (\sigma/r)^6 P_2(\cos\theta), \tag{4}$$

where the indices 1 and 2 refer to the absorber and the perturber, Q is the quadrupole of C_2H_2, A_2 is an adjustable effective parameter, P_2 is the second-order Legendre polynomial and θ is the angle between the C_2H_2 axis and the intermolecular axis. It should be noted that A_2 is often taken as γ_1, the reduced anisotropic component of the polarizability of the absorber [34]. Note that the short-range interaction in $R_2 r^{-12}$ of the Tipping–Herman potential [34] provides a negligible contribution even at high m values and has not been considered in this study. Moreover, the same angular dependence assumed for the attractive and repulsive parts of this potential leads to a negative cross-term contribution from $A_2 R_2$ [34] which has a comparable influence in $S_2(b)$ to the positive contribution from R_2^2. The contribution of the hexadecapole moment Φ has also been estimated by considering the total anisotropic potential

$$V_{\text{aniso}} = V_{Q_1Q_2} + V_{Q_1\Phi_2} + V_{\Phi_1Q_2} + V_{\Phi_1\Phi_2} - 4\varepsilon A_2 (\sigma/r)^6 P_2(\cos\theta). \tag{5}$$

In the calculation of line shifts, as well as the (weak) vibrational dependence of the self-broadenings, we consider only the vibrational dependence of the isotropic part of the potential V_{iso} which is, to our

knowledge, not available for any vibrational motion of C_2H_2. By assuming that V_{iso} is described by a 6–12 Lennard–Jones (LJ) model such as

$$V_{iso} = \frac{C_{12}}{r^{12}} - \frac{C_6}{r^6}, \quad \text{with } C_{12} = 4\varepsilon\sigma^{12} \text{ and } C_6 = 4\varepsilon\sigma^6, \tag{6}$$

the vibrational dephasing contribution is obtained from [31,35,36]

$$S_1^{iso} = \frac{3}{2}\frac{\Delta C_6}{C_6}\frac{\pi\varepsilon\sigma}{\hbar v_c'}\left[-\left(\frac{\sigma}{r_c}\right)^5 + \frac{21}{32}\left(\frac{\sigma}{r_c}\right)^{11} y\right]. \tag{7}$$

Here r_c is the distance of closest approach of the equivalent straight-path trajectory described with apparent velocity v_c', $\Delta C_6 = (C_6)_{v_f} - (C_6)_{v_i}$ and $y = (\Delta C_{12}/C_{12})/(\Delta C_6/C_6)$. The parameters $\Delta C_6/C_6$ and y are not known and are estimated from experimental results.

Self-broadening (γ_0 in $cm^{-1}\,atm^{-1}$) and shifting coefficients at different temperatures have been computed for the $\nu_1+\nu_2+\nu_4+\nu_5$ band of C_2H_2 by including the contributions of the perturber in the ground state with J_2 values up to 52 ($T = 296$ K). As a first step, we used the mean relative velocity (MV) that reduces the first integral in Equation (2) to one. Then we have considered the distribution of relative velocities (DV) by using 66 values of x from 0 to 10 with five different steps (0.02 from 0.04 up to 0.20, 0.05 up to 1.0, 0.10 up to 3.0, 0.2 up to 5 and 0.5 up to 10) so that the integral of $x e^{-x} dx = 1.00006$. Following the method described in Ref. [37], care was taken to discard any contribution of orbiting collisions corresponding to bound translational states. These contributions are very important at low relative velocities.

The fixed parameters used in the calculations are given in Table 1. We present below the results for the broadening coefficients for the R-branch only, since the results are practically the same for the P-branch, i.e. only very slightly smaller at high m values. It should also be noted that the parameters $\Delta C_6/C_6$ and y have almost no influence on the results of broadenings [35], which are first presented independently of the line shifts.

3. Theoretical results for the broadening and shifting coefficients and comparisons with experimental data

3.1. *Pressure broadening and shifting coefficients at 296 K*

The literature values for the quadrupole moment of C_2H_2 range from 3 to 8.4 D Å [40]. For the first calculation of self-broadening coefficients (γ_0 in cm^{-1} atm^{-1}), we have considered the experimental determination $Q = 5.42$ D Å [41] associated with $A_2 = \gamma_1 = 0.18$ [40]. Note that other experimental and calculated larger values of this quadrupole moment have been reported in Ref. [42] such as 6.15 D Å [43] and 6.53 D Å [44]. The results shown in Figure 1(a) are notably greater than the experimental data for middle and large m values ($m = J+1$ in the R-branch). This discrepancy is not surprising since for molecules with strong dipole and/or quadrupole moments, such as CO_2 [45], CH_3Cl [46], CH_3F [47] and CH_3Br [48], the self-broadening coefficients calculated from the most accurate values of the electric moments are generally overestimated. Then, using the same potential defined by Equation (4) with $Q = 5.0$ D Å and $A_2 = 0.50$, the results (Figure 1(a)) agree well with the experimental results for $m < 10$ but are still significantly larger for higher m. Finally, the parameters $Q = 4.5$ D Å and $A_2 = 0.60$ provide the best overall agreement with measurements (Figure 1(a)), although the results are too small for m values around 3–9. In the following, we shall consider mainly the parameters $Q = 4.5$ D Å and $A_2 = 0.60$.

As shown in Figure 1(b), the dispersion energy only has a significant contribution at low m values ($m < 7$). The total anisotropic potential defined by Equation (5) with an arbitrary hexadecapole moment $\Phi = 10$ D Å^3 yields slightly larger broadening coefficients at high m values. Note that the literature value from a quantum calculation, $\Phi = 21.8$ D Å^3 [49], is probably overestimated since the same quantum calculation also leads to an overestimated quadrupole moment of C_2H_2 ($Q = 7.35$ D Å).

Consideration of the Maxwell–Boltzmann velocity distribution leads to somewhat different results, in better agreement with the experimental data for $m = 6$–10, but at high m values these results (especially those

Table 1. Parameters used in the calculation of self-broadening and self-shifting coefficients in the $\nu_1+\nu_2+\nu_4+\nu_5$ band of $^{12}C_2H_2$.

B_i (cm^{-1})	B_f (cm^{-1})	D_i (10^{-6} cm^{-1})	D_f (10^{-6} cm^{-1})	ε (K)	σ (Å)
1.17664598	1.16797695	1.62421688	4.01615457	185	4.211

Note: The rotational parameters are taken from Ref. [38] and the Lennard–Jones parameters from Ref. [39].

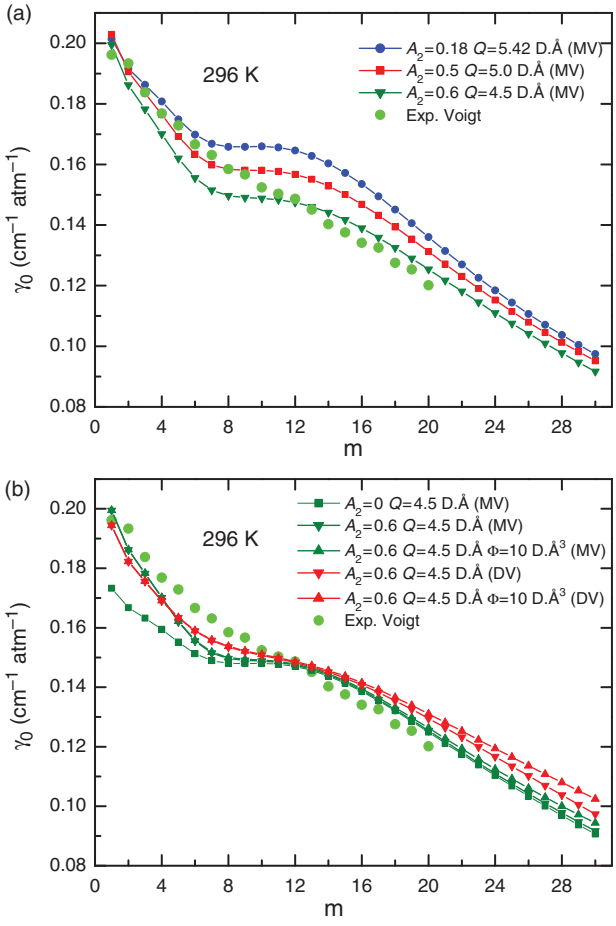

Figure 1. Self-broadening coefficients γ_0 in the $\nu_1+\nu_2+\nu_4+\nu_5$ band of $^{12}C_2H_2$ at 296 K. (a) The theoretical curves result from the mean relative velocity (MV) and different values of the parameter A_2 and the quadrupole moment Q. The experimental values [1] are derived from the Voigt profile. (b) The theoretical curves result from the mean velocity (MV) or the distribution of velocities (DV) and the given values of A_2, Q and the hexadecapole moment Φ.

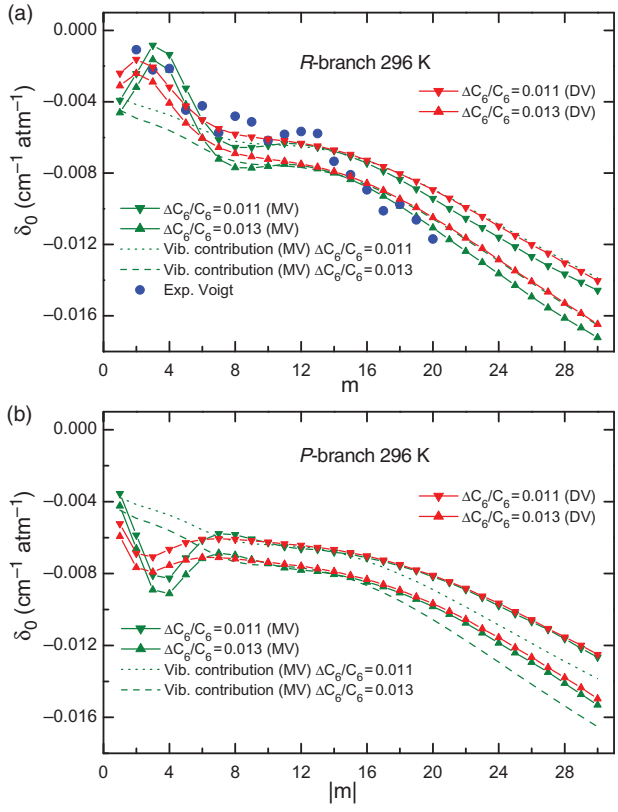

Figure 2. Self-shifting coefficients δ_0 in the R-branch (a) and P-branch (b) of the $\nu_1+\nu_2+\nu_4+\nu_5$ band of $^{12}C_2H_2$ at 296 K. The experimental values [1] are derived from measurements assuming the Voigt profile. The theoretical curves result from the mean velocity (MV) or the averaging over the distribution of velocities (DV) and the anisotropic potential defined by Equation (4) with $Q=4.5$ D Å, $A_2=0.6$ and $y=1$ and the given values of $\Delta C_6/C_6$.

including the contribution of the hexadecapole moment) are significantly larger than the experimental values.

The pressure-induced line shift coefficients (δ_0 in cm^{-1} atm^{-1}) have been calculated at 296 K with a fixed y parameter ($y=1$) and two adjusted values of $\Delta C_6/C_6$, i.e. 0.011 and 0.013 (Figure 2(a) for the R-branch and Figure 2(b) for the P-branch). In the R-branch, the latter value of $\Delta C_6/C_6$ provides satisfactory results only at large m values, whereas the best overall agreement between the theoretical and measured pressure shifts is obtained using $\Delta C_6/C_6=0.011$. The total calculated line shift results from two contributions, namely a 'vibrational' dephasing contribution (given by Equation (11) of Ref. [35]), which has a rotational dependence through the real part of S_2^{aniso}, and a rotational contribution involving its imaginary part (see Equation (4) of Ref. [36]). The vibrational contribution (for which Im S_2^{aniso} is neglected) is nearly identical in the two branches. The rotational contribution (including the weak vibrational dependence of the rotational constants in the final vibrational level) is derived from Im S_2^{aniso} where S_1^{iso} is neglected.

By comparing the vibrational dephasing contribution (written in condensed notation as 'vib.' contribution in the figures) with the total line shifts (Figure 2), it appears that the rotational contribution is only significant for $|m|$ ranging from 2 to 6 and induces a strong asymmetry in the shifts of these lines in the P- and R-branches. Indeed, the rotational contribution has roughly the same magnitude in a P(J) line and an R(J–1) line with opposite signs, which explains this asymmetry [50]. Consideration of the velocity distribution provides, at low m values, a

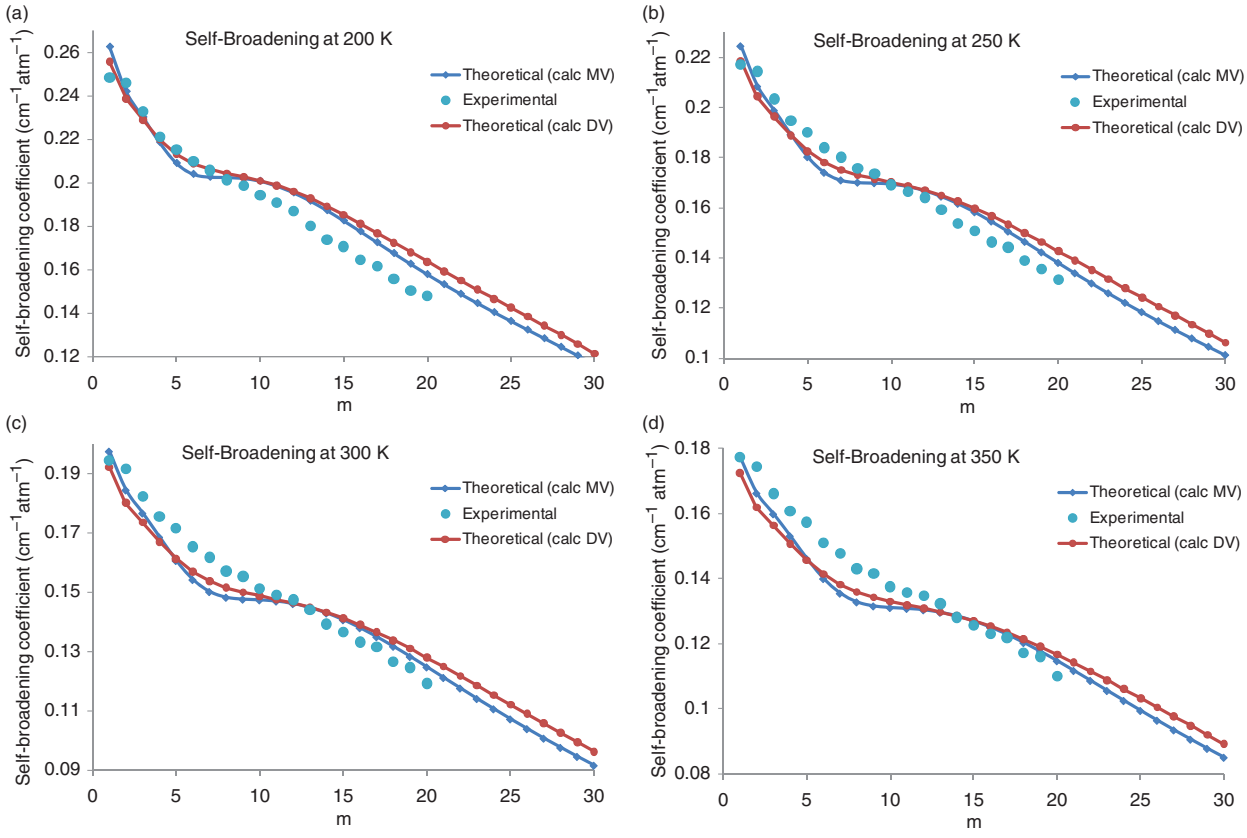

Figure 3. Self-broadening coefficients γ_0 in the $\nu_1+\nu_2+\nu_4+\nu_5$ band of $^{12}C_2H_2$ at 200 K (a), 250 K (b), 300 K (c) and 350 K (d). The experimental values are evaluated from measurements at different temperatures [1] assuming the Voigt profile. The theoretical curves result from the anisotropic potential defined by Equation (4) with $Q=4.5$ D Å and $A_2=0.6$, and the mean velocity (MV) or averaging over the distribution of velocities (DV).

smaller bump in the R-branch than the calculation with MV, as well as a shallower dip in the P-branch with a slightly smaller magnitude of the line shifts at large $|m|$.

3.2. *Pressure broadening and shifting coefficients at 200, 250, 300, and 350 K*

The self-broadening and self-shift coefficients have been computed for $T=200$, 250, 300 and 350 K using the parameter values $Q=4.5$ D Å and $A_2=0.6$, $\Delta C_6/C_6=0.011$ and $y=1$ (Figures 3 and 4). The results from MV and DV are close and present similar differences at the four temperatures. Comparison of theoretical broadening coefficients γ_0(calc) with experimental data at the same temperature γ_0(exp) derived from measurements shows the following features. At 200 K, γ_0(calc) agrees well with γ_0(exp) for low m ($m<10$), and is somewhat larger for higher m; at 250 K, there is overall agreement: γ_0(calc) is slightly smaller than γ_0(exp) for $m<10$ and slightly larger for $m>10$; as T rises from 300 to 350 K the discrepancy for $m<10$ increases, and the agreement at higher m is improved. Then, the best agreement between γ_0(calc) and γ_0(exp), arising from the quadrupole moment considered for C_2H_2, is shifted towards high m values as T increases, and the dispersion energy considered is probably too simple to provide satisfactory agreement at room or high temperatures for low m values ($1<m<10$). It should be noted that the resonance condition [51] for the quadrupole–quadrupole interaction is obtained for $J_i\approx J_{2\max}$, where $J_{2\max}$ is the most populated level of the perturber at the temperature considered. $J_{2\max}$ increases from 7 for $T=200$ K to 11 for $T=350$ K and the higher levels of the transition are more populated as T increases.

As shown in Figure 4, the theoretical line shift coefficients δ_0(calc) in the R-branch at 200, 250, 300, and 350 K are in overall agreement with experimental data δ_0(exp) at the same temperatures derived from measurements. They decrease in magnitude (as the broadening coefficients) as T increases because the gas

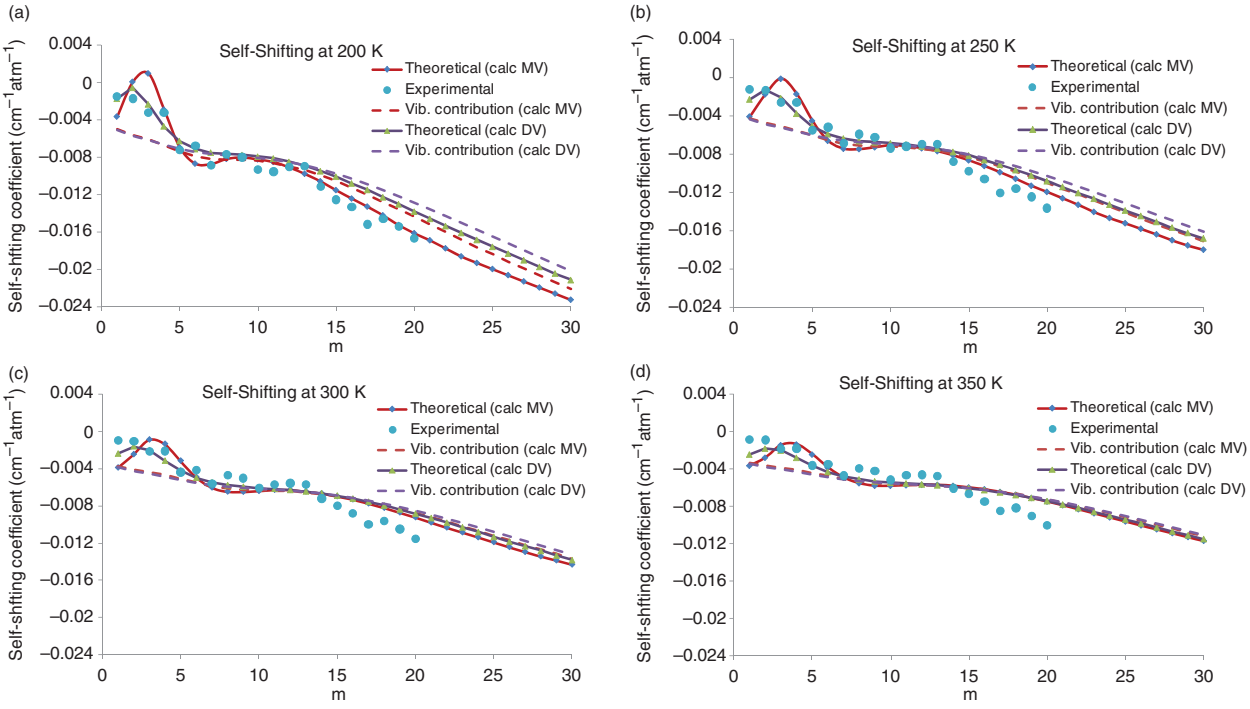

Figure 4. Self-shifting coefficients δ_0 in the R-branch of the $\nu_1+\nu_2+\nu_4+\nu_5$ band of $^{12}C_2H_2$ at 200 K (a), 250 K (b), 300 K (c) and 350 K (d). The experimental values are evaluated from measurements at different temperatures [1] assuming the Voigt profile. The theoretical curves result from the anisotropic potential defined by Equation (4) with $Q=4.5$ D Å and $A_2=0.6$, the isotropic LJ potential (Equation (6)) with $\Delta C_6/C_6=0.011$ and $y=1$, and the mean velocity (MV) or averaging over the distribution of velocities (DV).

density is then smaller at constant pressure (1 atm); for $m>3$, they also roughly increase with m, due to the vibrational dephasing contribution increasing smoothly with m and the vanishing rotational contribution. The comparison between δ_0(calc) and δ_0(exp) shows the same behavior for all temperatures considered: the curves δ_0(calc) versus m present a bump for m between 1 and 5 due to the rotational contribution, which is much less pronounced for DV than for MV, in agreement with the data, and rather good agreement is obtained for m between 5 and 15; the theoretical curves are smaller in magnitude than the experimental data for higher m. It should also be noted that the differences between the results derived from MV and DV are significantly reduced as T increases.

4. Temperature dependence of broadening and shifting coefficients

4.1. *Temperature dependence of self-broadening coefficients*

The temperature dependence of the broadening coefficients is usually well represented by the simple power law given by Equation (9) of Ref. [1]. For a constant pressure of 1 atm at any temperature considered, this equation becomes

$$\gamma_0(T)=\gamma_0(T_0)\left[\frac{T_0}{T}\right]^n, \tag{8}$$

where $T_0=296$ K is our reference temperature. The n exponent values were determined [1] by comparing the measured values of $\gamma_0(T)$ derived from the Voigt and speed-dependent Voigt profile for T in the range 213–333 K. The experimental broadening coefficients were then calculated at 200, 250, 300 and 350 K from these n values. Assuming non-independent errors in the broadening measurements which are obtained from the same spectrometer, the uncertainty in n was estimated to be about ±0.03. The experimental values of n lie between 0.57 and 0.63 for $m\leq11$ and decrease significantly at higher m values.

The theoretical n values have been evaluated from the calculated γ_0 values at 200, 250, 300, and 350 K. As shown in Figure 5, the relation between $\ln\gamma_0(T)$ and $\ln(T_0/T)$ is quite linear, which justifies *a posteriori* the use of the empirical power law defined by Equation (8). The n exponent is given by the slope of the straight line obtained for each m value. The results (with

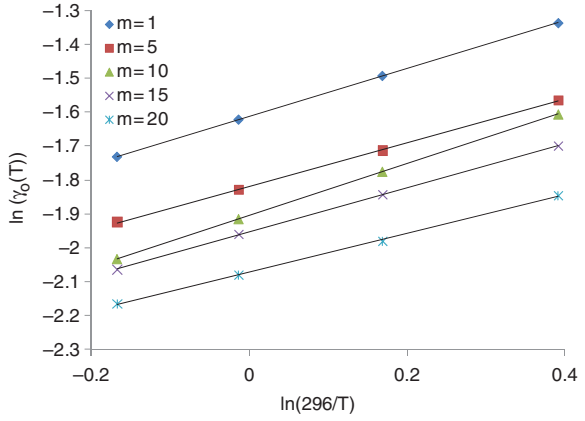

Figure 5. Theoretical temperature dependence of C_2H_2 self-broadening coefficients for $m = 1$, 5, 10, 15 and 20.

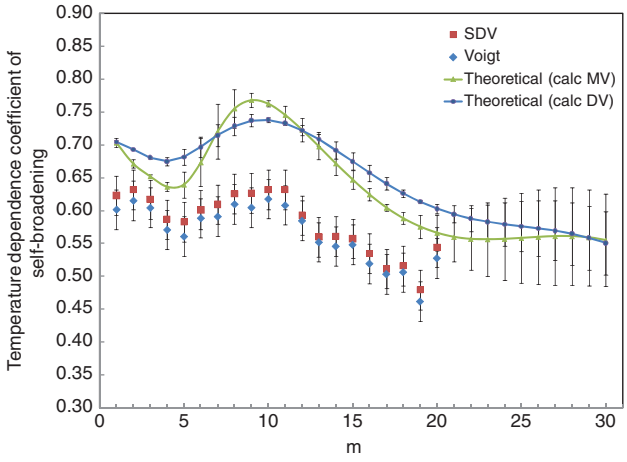

Figure 6. Variation of the temperature dependence exponent n with m for the self-broadening coefficients of C_2H_2 in the $\nu_1+\nu_2+\nu_4+\nu_5$ band. The experimental results with error bars are derived from Voigt and speed-dependent Voigt (SDV) profiles. The solid curves (with error bars corresponding to 3SD) represent the theoretical results calculated with the mean velocity (MV) or averaging over the distribution of velocities (DV).

uncertainty bars arbitrarily set to 3SD of these slopes) derived from the calculated broadening coefficients involving the velocity distribution are significantly different to those derived from the average velocity. As shown in Figure 6 the curve $n(m)$ calculated from DV has less prominent variations than the curve calculated from MV. Figure 6 and Table 2 show a comparison of these results with experimental results derived from Voigt and speed-dependent Voigt profiles. In view of the experimental and theoretical uncertainties the theoretical n values are significantly larger for m ranging from 7 to 19 than the experimental results. Note, however, that the curves $n(m)$ present the same behavior, with first a decrease (up to $m = 4$ or 5), then an increase (up to $m = 9$ or 11) and finally a decrease for higher m. For $m \approx 9$, corresponding to the resonant condition of the quadrupole–quadrupole interaction, the theoretical exponent is close to 0.75, as predicted by Birnbaum [52] for this interaction. It should also be noted that the standard deviations and thus the error bars for n values (DV) are generally smaller than for n values (MV) and these errors become much larger for $m > 20$.

4.2. *Temperature dependence of self-shift coefficients*

In the preceding paper [1] we employed two empirical laws given by Equations (11) and (12) of Ref. [1] to derive the temperature dependence of self-line shift coefficients. The power law described by Equation (12) cannot be used here to calculate this dependence theoretically since this law is unable to predict negative and positive line shifts depending on m. Actually, the calculated line shifts δ_0 are generally negative, except for two lines, R(1) and R(2), of C_2H_2 at 200 K calculated with MV. Therefore, we first used the linear temperature dependence defined by Equation (11) of Ref. [1], i.e.

$$\delta_0(T) = \delta_0(T_0) + \delta_0'(T - T_0). \tag{9}$$

Typical results of δ_0 vs. T are represented in Figure 7 for $T = 200$, 250, 300, and 350 K. The linear dependence is generally inaccurate for any calculations derived from MV or DV. Nevertheless, we have fitted all the shifts according this equation in order to compare the theoretical and experimental temperature dependences. The resulting δ_0'(MV or DV) coefficients are given in Table 3 and Figure 8 where the uncertainty bars correspond to three times the standard deviation derived from the linear least-squares procedures. These standard deviations (SDs) are very large in relative value, except for the lines R(6), R(7) and R(8) calculated using MV.

Figure 8 also shows the δ_0'(vib) coefficients derived from the vibrational dephasing contribution to the theoretical (MV) line shifts and the δ_0'(exp) coefficients derived from the experimental results for the line shifts. It appears that the SDs of δ_0'(vib) are significantly smaller than the SDs of δ_0'(MV) for low m ($m < 7$), which means that the lack of accuracy in the linear model of Equation (9) arises mainly from the rotational contribution calculated with MV. That contribution also explains the dip and bump around $m = 2$–3 and $m = 5$–6, respectively. The dip is well observed experimentally and is indeed much deeper, but not

Table 2. Self-broadening coefficients γ_0 ($cm^{-1}\,atm^{-1}$) at 296 K and their temperature dependence exponents n. The experimental results γ_0(exp) and n(exp) are derived from measurements assuming the Voigt lineshape [1]. The calculated results γ_0(MV) and γ_0(DV) are derived from the average velocity and the distribution of velocities, respectively. The values quoted in parentheses for the theoretical exponents n are one standard deviation (see text).

Line	m	γ_0(exp)	γ_0(MV)	γ_0(DV)	n(exp)	n(MV)	n(DV)
R(0)	1	0.1962 (2)	0.1994	0.1944	0.62(3)	0.703(2)	0.704(1)
R(1)	2	0.1933 (2)	0.1862	0.1823	0.63(3)	0.672(2)	0.693(0)
R(2)	3	0.1837 (2)	0.1782	0.1756	0.62(3)	0.652(1)	0.681(1)
R(3)	4	0.1768 (2)	0.1701	0.1690	0.59(3)	0.636(2)	0.675(2)
R(4)	5	0.1728 (2)	0.1620	0.1633	0.58(3)	0.640(7)	0.681(4)
R(5)	6	0.1666 (2)	0.1555	0.1589	0.60(3)	0.673(12)	0.697(5)
R(6)	7	0.1631 (2)	0.1515	0.1557	0.61(3)	0.721(14)	0.715(6)
R(7)	8	0.1584 (2)	0.1497	0.1535	0.63(3)	0.755(10)	0.729(5)
R(8)	9	0.1566 (2)	0.1491	0.1520	0.63(3)	0.768(4)	0.737(3)
R(9)	10	0.1524 (2)	0.1488	0.1507	0.63(3)	0.763(0)	0.738(1)
R(10)	11	0.1503 (2)	0.1484	0.1496	0.63(3)	0.746(4)	0.733(1)
R(11)	12	0.1486 (1)	0.1475	0.1483	0.59(3)	0.723(6)	0.722(3)
R(12)	13	0.1451 (1)	0.1461	0.1468	0.56(3)	0.698(6)	0.708(4)
R(13)	14	0.1402 (1)	0.1442	0.1451	0.56(3)	0.672(6)	0.692(4)
R(14)	15	0.1375 (1)	0.1418	0.1431	0.56(3)	0.647(5)	0.675(5)
R(15)	16	0.1341 (1)	0.1390	0.1408	0.53(3)	0.625(3)	0.657(4)
R(16)	17	0.1325 (1)	0.1359	0.1382	0.51(3)	0.604(2)	0.641(3)
R(17)	18	0.1275 (1)	0.1325	0.1355	0.52(3)	0.588(3)	0.626(2)
R(18)	19	0.1253 (1)	0.1290	0.1326	0.48(2)	0.576(6)	0.614(1)
R(19)	20	0.1201 (1)	0.1254	0.1295	0.54(3)	0.566(9)	0.603(2)
R(20)	21		0.1218	0.1264		0.560(12)	0.594(4)
R(21)	22		0.1181	0.1232		0.557(16)	0.588(7)
R(22)	23		0.1145	0.1199		0.556(19)	0.583(9)
R(23)	24		0.1110	0.1167		0.557(21)	0.579(11)
R(24)	25		0.1075	0.1134		0.558(23)	0.576(13)
R(25)	26		0.1042	0.1096		0.560(24)	0.573(14)
R(26)	27		0.1009	0.1070		0.561(25)	0.569(15)
R(27)	28		0.0978	0.1037		0.561(25)	0.565(16)
R(28)	29		0.0947	0.1005		0.559(24)	0.559(16)
R(29)	30		0.0917	0.0973		0.555(23)	0.551(16)

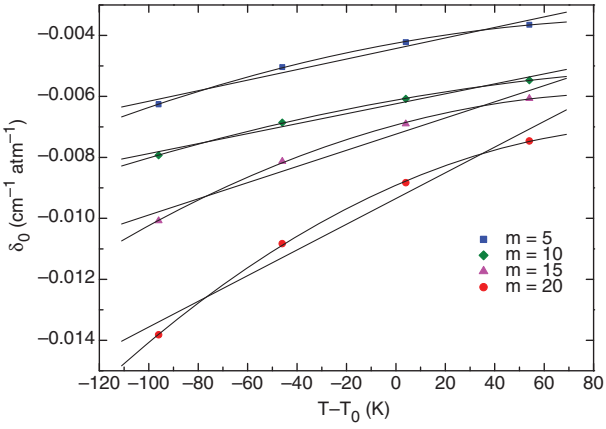

Figure 7. Theoretical temperature dependence of C_2H_2 self-shift coefficients δ_0 calculated from the distribution of velocities for $m = 5$, 10, 15 and 20. The straight lines are obtained from a linear fit and the curves from a quadratic least-squares procedure. The reference temperature T_0 is 296 K.

the bump. The dip and bump are much less pronounced for the δ_0'(DV) coefficients, which are also notably smaller than δ_0'(MV) for large m values. It should be noted that, except for the bump around $m = 5$–6, reasonable agreement is obtained with the experimental results, which increase with m from $m = 3$. Note also that the SDs of δ_0'(vib) are comparable to the SDs of δ_0'(MV or DV) as m increases since the vibrational contribution becomes predominant in the line shifts.

The coefficients δ_0'(DV), with SDs generally smaller than those of δ_0'(MV), lead only through Equation (9) only to a rough evaluation of $\delta_0(T)$ from $\delta_0(T_0)$. Therefore, we also used a quadratic temperature dependence of the self-induced shifts given by

$$\delta_0(T) = \delta_0(T_0) + \delta_0'(T - T_0) + \delta_0'' \frac{(T - T_0)^2}{2}. \quad (10)$$

Table 3. Self-shifting coefficients δ_0 ($10^{-3}\,cm^{-1}\,atm^{-1}$) at 296 K and the temperature dependence parameters δ'_0 ($10^{-5}\,cm^{-1}\,atm^{-1}\,K^{-1}$) and δ''_0 ($10^{-7}\,cm^{-1}\,atm^{-1}\,K^{-2}$). The experimental results δ_0(exp) and δ'_0(exp) are derived from measurements assuming the Voigt lineshape [1]. The parameters δ_0(MV) and δ_0(DV) are calculated using the mean velocity and the distribution of velocities, respectively. The parameters δ'_0(MV) and δ'_0(DV) are calculated from Equation (9). The parameters of the last columns δ_0, δ'_0, δ''_0(DV) are calculated from Equation (10). The values quoted in parentheses for the calculated parameters are one standard deviation (see text).

Line	δ_0(exp)	δ_0(MV)	δ_0(DV)	δ'_0(exp)	δ'_0(MV)	δ'_0(DV)	δ_0, δ'_0, δ''_0(DV)
R(0)		−3.92	−2.40		0.04(20)	−0.47(15)	−2.43(3) −0.27(5) 0.92(16)
R(1)	−1.08(1)	−2.43	−1.62	0.5(1)	−1.86(45)	−0.84(16)	−1.62(2) −0.63(4) 0.98(12)
R(2)	−2.21(1)	−0.84	−2.06	−4.6(2)	−1.61(14)	0.20(6)	−2.04(2) 0.12(3) −0.36(9)
R(3)	−2.14(1)	−1.36	−3.18	−1.2(1)	1.00(42)	1.23(19)	−3.18(3) 0.99(5) −1.18(17)
R(4)	−4.47(2)	−3.24	−4.24	−1.6(1)	2.97(57)	1.73(21)	−4.25(3) 1.46(4) −1.30(13)
R(5)	−4.23(2)	−5.02	−5.02	0.8(1)	3.24(34)	1.85(18)	−5.04(2) 1.62(2) −1.14(8)
R(6)	−5.70(3)	−6.13	−5.51	0.6(1)	2.56(8)	1.79(15)	−5.53(2) 1.59(2) −0.96(7)
R(7)	−4.81(2)	−6.56	−5.82	1.9(1)	1.79(7)	1.69(13)	−5.84(2) 1.52(2) −0.82(8)
R(8)	−5.10(3)	−6.56	−5.98	2.6(1)	1.49(3)	1.61(12)	−6.00(2) 1.45(2) −0.78(8)
R(9)	−6.17(3)	−6.46	−6.10	2.8(1)	1.59(21)	1.63(15)	−6.12(2) 1.44(3) −0.92(11)
R(10)	−5.80(3)	−6.33	−6.19	3.6(2)	1.83(28)	1.70(17)	−6.21(2) 1.48(4) −1.08(13)
R(11)	−5.67(3)	−6.37	−6.33	1.5(1)	2.25(37)	1.88(22)	−6.33(3) 1.59(5) −1.36(18)
R(12)	−5.78(3)	−6.55	−6.48	1.6(1)	2.69(44)	2.08(26)	−6.48(5) 1.74(7) −1.62(24)
R(13)	−7.30(4)	−6.75	−6.70	5.8(3)	3.16(53)	2.37(31)	−6.69(5) 1.97(8) −1.94(26)
R(14)	−8.09(4)	−7.08	−6.95	3.8(2)	3.66(62)	2.65(36)	−6.94(5) 2.18(9) −2.24(28)
R(15)	−8.90(4)	−7.44	−7.28	4.1(2)	4.13(67)	2.99(40)	−7.26(6) 2.46(10) −2.50(32)
R(16)	−10.11(5)	−7.89	−7.63	4.8(2)	4.53(68)	3.29(43)	−7.61(6) 2.72(10) −2.72(34)
R(17)	−9.74(5)	−8.36	−8.04	3.5(2)	4.95(71)	3.62(47)	−8.02(6) 3.01(10) −2.94(34)
R(18)	−10.62(5)	−8.89	−8.46	4.2(2)	5.41(76)	3.92(49)	−8.44(6) 3.27(10) −3.10(34)
R(19)	−11.69(6)	−9.42	−8.94	3.7(2)	5.73(79)	4.22(52)	−8.91(6) 3.54(10) −3.24(32)
R(20)		−9.99	−9.41		5.97(77)	4.49(53)	−9.39(6) 3.78(10) −3.36(34)
R(21)		−10.54	−9.93		6.26(79)	4.75(54)	−9.91(6) 4.03(10) −3.42(32)
R(22)		−11.06	−10.43		6.56(79)	4.97(56)	−10.40(6) 4.24(10) −3.50(32)
R(23)		−11.60	−10.97		6.74(78)	5.20(57)	−10.92(6) 4.45(10) −3.56(32)
R(24)		−12.13	−11.50		6.87(79)	5.42(57)	−11.44(6) 4.66(10) −3.60(32)
R(25)		−12.68	−12.01		7.02(78)	5.62(59)	−11.94(8) 4.84(13) −3.72(42)
R(26)		−13.20	−12.50		7.19(78)	5.80(60)	−12.46(6) 5.01(9) −3.76(30)
R(27)		−13.66	−13.04		7.36(76)	6.00(61)	−12.96(7) 5.19(9) −3.86(30)
R(28)		−14.12	−13.52		7.52(80)	6.18(63)	−13.46(7) 5.34(12) −3.98(38)
R(29)		−14.57	−14.03		7.67(85)	6.38(65)	−13.94(9) 5.52(13) −4.10(42)

As shown in Figure 7, this quadratic dependence of $\delta_0(T)$ allows us to fit much more accurately the calculated self-shift coefficients than the linear dependence. The coefficients δ_0, δ'_0 and δ''_0 determined through the fit of the calculated line shifts with DV at 200, 250, 300, and 350 K are given in the last columns of Table 3. The new δ'_0 coefficients, shown in Figure 8 with error bars also set to 3SD, are notably different to the previous linear coefficients derived from MV and Equation (9), and their SDs are on average six times smaller. They are in good agreement with the same coefficients calculated with DV from Equation (9) for $m < 12$ and slightly smaller for higher m. The quadratic polynomial (Equation (10)) enables the calculation of $\delta_0(T)$ at any temperature between 200 and 350 K from the values of δ_0, δ'_0 and δ''_0 (last columns of Table 3) with an accuracy (with respect to the results of the direct calculation) less than or equal to the SDs of the coefficient δ_0. Note that the δ_0 values listed in columns 3 and 4 of Table 3 are those calculated directly with MV and DV at 296 K, whereas the δ_0 values with their SD in column 8 correspond to the fitted value for $T = 296$ K.

5. Conclusion

We have calculated the self-broadening coefficients and self-shift coefficients in the $\nu_1+\nu_2+\nu_4+\nu_5$ band of C_2H_2 first at 296 K and then at four temperatures ranging from 200 to 350 K and compared them with previous experimental measurements [1]. The calculations were performed using a semiclassical model involving only two interactions: the strong electrostatic quadrupole–quadrupole interaction and an empirical dispersion contribution significant only at low m values.

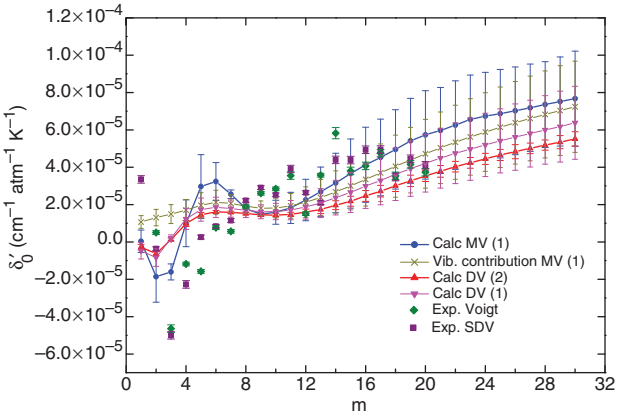

Figure 8. Temperature dependence coefficient δ'_0 for the self-broadening coefficients of C_2H_2 in the $\nu_1+\nu_2+\nu_4+\nu_5$ band. The experimental results with error bars are derived from Voigt and speed-dependent Voigt (SDV) profiles. The curves (with error bars corresponding to 3SD) represent the theoretical results derived from the mean velocity (MV), the distribution of velocities (DV) with a linear fit (1) defined by Equation (9) and a quadratic fit (2) defined by Equation (10) on the calculated δ_0 values.

This very simple intermolecular potential associated with a rather low value of the quadrupole moment of C_2H_2 (4.5 D Å) leads to results for broadening coefficients in overall agreement with the experimental data at any temperature considered. Slightly different results are obtained using the mean relative velocity and the Maxwell–Botzmann distribution of relative velocities.

The theoretical temperature dependence exponents of the self-broadening coefficients were also determined from calculated results at 200, 250, 300 and 350 K. They are significantly different using the average velocity or the distribution of velocities and they are notably larger than the exponent values derived from measurements of broadening coefficients for a comparable temperature range. Note, however, that the theory reproduces roughly the rotational dependence of these experimental n values.

The vibrational dependence of the isotropic part of the potential including mainly one adjustable parameter can well predict the general behavior of the line shifts that increase in magnitude with m. Note that we have neglected in this calculation the vibrational dependence of the anisotropic part of the potential. The rotational contribution, which is only significant for m ranging from 2 to 5 and notably depends on the MV or DV calculation, roughly explains the small line shifts observed at low m values in the R-branch. There is a similar overall agreement between the measured and theoretical variations of the self-shift coefficients at the four temperatures considered. Although the empirical linear temperature dependence of the theoretical line shifts is not satisfactory and significantly different from MV or DV calculations, the resulting δ'_0 coefficients agree more or less with those derived from the measurements of line shifts for middle or high m values. We have shown that the theoretical variation of the temperature is well reproduced by a quadratic polynomial. If we discard plausible large experimental uncertainties in the δ'_0 coefficients at low m values, the disagreement with theoretical results for these m values could be partly due to the calculation of the rotational contribution of the shifts. Note that the theoretical model includes only second-order terms in the development of the semiclassical S matrix.

Acknowledgements

A. Predoi-Cross acknowledges financial support from the Natural Sciences and Engineering Research Council of Canada, and University of Lethbridge Research Funds. The authors are very grateful to Dr F. Thibault for stimulating discussions, bringing several references to our attention, and his assistance in improving the manuscript.

References

[1] C. Povey, A. Predoi-Cross and D.R. Hurtmans, J. Mol. Spectrosc., **268**, 177 (2011).
[2] R.A. Whitby and E.R. Altwicker, Atmos. Environ. **12**, 1289 (1978).
[3] P.V. Sada, G.L. Bjoraker, D.E. Jennings, G.H. McCabe and P.N. Romani, Icarus **136**, 192 (1998).
[4] J.I. Moses, B. Bézard, E. Lellouch, G. Randall Gladstone, H. Feuchtgruber and M. Allen, Icarus **143**, 244 (2000).
[5] D. Horn, J.M. McAfee, A.M. Winer, K.C. Herr and G.C. Pimentel, Icarus **16**, 543 (1972).
[6] R.J. Vervack Jr, B.R. Sandel and D.R. Strobel, Icarus **170**, 91 (2004).
[7] A. Babay, M. Ibrahimi, V. Lemaire, B. Lemoine, F. Rohart and J.P. Bouanich, J. Quant. Spectrosc. Radiat. Transfer **59**, 195 (1998).
[8] J.P. Bouanich, J. Walrand and G. Blanquet, J. Mol. Spectrosc. **219**, 98 (2003).
[9] B. Lance, G. Blanquet, J. Walrand and J.P. Bouanich, J. Mol. Spectrosc. **185**, 262 (1997).
[10] J.L. Domenech, F. Thibault, D. Bermejo and J.P. Bouanich, J. Mol. Spectrosc. **225**, 48 (2004).
[11] D. Lambot, G. Blanquet, J. Walrand and J.P. Bouanich, J. Mol. Spectrosc. **150**, 164 (1991).
[12] F. Thibault, B. Corretja, A. Viel, D. Bermejo, R.Z. Martinez and B. Bussery-Honvault, Phys. Chem. Chem. Phys. **10**, 5419 (2008).
[13] F. Thibault, E.P. Fuller, K.A. Grabow, J.L. Hardwick, C.I. Marcus, D. Marston, L.A. Roberston,

E.N. Senning, M.C. Stoffel and R.S. Wilser, J. Mol. Spectrosc. **256**, 17 (2009).
[14] D. Lambot, G. Blanquet and J.P. Bouanich, J. Mol. Spectrosc. **136**, 86 (1989).
[15] J.P. Bouanich, G. Blanquet, J.C. Populaire and J. Walrand, J. Mol. Spectrosc. **190**, 7 (1998).
[16] J.P. Bouanich, G. Blanquet and J. Walrand, J. Mol. Spectrosc. **194**, 269 (1999).
[17] J. Buldyreva and L. Nguyen, Mol. Phys. **102**, 1523 (2004).
[18] D. Lambot, A. Olivier, G. Blanquet, J. Walrand and J.P. Bouanich, J. Quant. Spectrosc. Radiat. Transfer **45**, 145 (1991).
[19] D. Lambot, J.C. Populaire, J. Walrand, G. Blanquet and J.P. Bouanich, J. Mol. Spectrosc. **165**, 1 (1994).
[20] D. Jacquemart, J.Y. Mandin, V. Dana, L. Régalia-Jarlot, X. Thomas and P. Van der Heyde, J. Quant. Spectrosc. Radiat. Transfer **75**, 397 (2002).
[21] M. Lepère, G. Blanquet, J. Walrand, J.P. Bouanich, M. Herman and J. Vander Auwera, J. Mol. Spectrosc. **242**, 25 (2007).
[22] A.S. Pine, J. Quant. Spectrosc. Radiat. Transfer. **50**, 149 (1993).
[23] F. Herregotds, D. Hurtmans, J. Vander Auwera and M. Herman, J. Chem. Phys. **111**, 7954 (1999).
[24] H. Valipour and D. Zimmerman, J. Chem. Phys. **114**, 3535 (2001).
[25] A. Lucchesini, M. de Rosa, D. Pelliccia, C. Gabbanini and S. Gozzini, Appl. Phys. B. **63**, 277 (1996).
[26] P. Varanasi and R.P. Bangaru, J. Quant. Spectrosc. Radiat. Transfer **15**, 267 (1975).
[27] J.S. Wong, J. Mol. Spectrosc. **82**, 449 (1980).
[28] C.P. McRaven, M.J. Cich, G.V. Lopez, T.J. Sears, D. Hurtmans and A.W. Mantz, J. Mol. Spectrosc. **266**, 43 (2011).
[29] R. Georges, D. Van Der Vorst, M. Herman and D. Hurtmans, J. Mol. Spectrosc. **185**, 187 (1997).
[30] D. Robert and J. Bonamy, J. Phys. **40**, 923 (1979).
[31] J.P. Bouanich, D. Bermejo, J.L. Domenech, R.Z. Martinez and J. Santos, J. Mol. Spectrosc. **179**, 22 (1996).
[32] J.P. Bouanich, C. Campers, G. Blanquet and J. Walrand, J. Quant. Spectrosc. Radiat. Transfer **39**, 353 (1988).
[33] J. Bonamy, L. Bonamy and D. Robert, J. Chem. Phys. **67**, 4441 (1977).
[34] R.H. Tipping and R.M. Herman, J. Quant. Spectrosc. Radiat. Transfer **10**, 881 (1970).
[35] F. Thibault, J. Boissoles, R. Le Doucen, J.P. Bouanich, P. Arcas and C. Boulet, J. Chem. Phys. **96**, 4945 (1992).
[36] J.L. Domenech, D. Bermejo and J.P. Bouanich, J. Mol. Spectrosc. **200**, 266 (2000).
[37] J.P. Looney and R.M. Herman, J. Quant. Spectrosc. Radiat. Transfer **37**, 547 (1987).
[38] M. Herman, Mol. Phys. **105**, 2217 (2007).
[39] J.O. Hirschfelder, C.F. Curtiss and R.B. Bird, *Molecular Theory of Gases and Liquids* (Wiley, New York, 1967).
[40] C.G. Gray and K.E. Gubbins, *Theory of Molecular Fluids* (Oxford University Press, New York, 1984).
[41] I.R. Dagg, A. Anderson, W. Smith, M. Missio, C.G. Joslin and L.A.A. Read, Can. J. Phys. **66**, 453 (1988).
[42] J.M. Junquera-Hernandez, J. Sanchez-Marin and D. Maynau, Chem. Phys. Lett. **359**, 343 (2002).
[43] S. Coriani, C. Hättig, P. Jorgensen, A. Rizzo and K. Ruud, J. Chem. Phys. **109**, 7176 (1998).
[44] A. Halkier and S. Coriani, Chem. Phys. Lett. **303**, 408 (1999).
[45] L. Rosenmann, J.M. Hartmann, M.Y. Perrin and J. Taine, J. Chem. Phys. **88**, 2999 (1988).
[46] G. Blanquet, J. Walrand, J.C. Populaire and J.P. Bouanich, J. Quant. Spectrosc. Radiat. Transfer **53**, 211 (1995).
[47] B. Lance, M. Lepère, G. Blanquet, J. Walrand and J.P. Bouanich, J. Mol. Spectrosc. **180**, 100 (1996).
[48] L. Gomez, D. Jacquemart, J.P. Bouanich, Z. Boussetta and H. Aroui, J. Quant. Spectrosc. Radiat. Transfer **111**, 1252 (2010).
[49] R.D. Amos and J.H. Williams, Chem. Phys. Lett. **66**, 471 (1979).
[50] C. Luo, R. Wehr, J.R. Drummond, A.D. May, F. Thibault, J. Boissoles, J.M. Launay, C. Boulet, J.P. Bouanich and J.M. Hartmann, J. Chem. Phys. **115**, 2198 (2001).
[51] M. Giraud, D. Robert and L. Galatry, C.R. Acad. Sci. Paris **272**, 1252 (1971).
[52] G. Birnbaum, Adv. Chem. Phys. **12**, 487 (1967).